Int. J. Advanced Design and Manufacturing Technology, 2023, Vol. 16, No. 3, pp. 71-87

DOI: 10.30486/admt.2023.1960808.1356 ISSN: 2252-0406 https://admt.isfahan.iau.ir

Active Control of Sandwich Microbeams Vibration with FGM and Viscoelastic/ER Core

Amir Hossein Yousefi
Department of Civil Engineering, Shahinshahr Branch, Islamic Azad University, Shahinshahr, Iran
E-mail: uosefi@shaiau.ac.ir

Farhad Kiani *
Department of Mechanical Engineering, Shahinshahr Branch, Islamic Azad University, Shahinshahr, Iran
E-mail: kiani@shaiau.ac.ir
*Corresponding author

Esmaeil Abedi
Department of Mechanical Engineering, Kashan Branch, Islamic Azad University, Kashan, Iran
E-mail: esmaeil.abedi@gmail.com

Received: 13 August 2022, Revised: 26 March 2023, Accepted: 10 March 2023

Abstract: This study is devoted to analyse of free and forced vibrations and semi-active control vibrations of sandwich microbeam with Functionally Graded Materials (FGM) and viscoelastic/electrorheological (ER) core. The intended model is for top and bottom layers of functionally graded materials with power law and a core model for Viscoelastic materials with complex shear modulus. Hamilton principle is used to determine the governing Equations of motion on the sandwich microbeam based on the modified couple stress theory. Mesh less method of Radial Basis Functions (RBF) is used to calculate natural frequency and the loss factor. All the effects of length scale parameter, shear modulus and changes due to variation of the electric field on the natural frequency and loss factor have been drawn. Combination of RBF method and forward difference led to evaluation of forced vibration and deflection of microbeam for length scale parameters and different electric fields under the dynamic load have been calculated and drawn. The feedback effects are analyzed for vibration amplitudes of sandwich microbeam by using Linear Quadratic Gaussian (LQG) and optimal control method. At the end, the results are compared with papers for different viscoelastic models such as Kelvin model, Bingham plastic model and complex modulus

Keywords: Electrorheological, FGM Faces, RBF, Sandwich Microbeam, Semi-Active Control, Viscoelastic

Biographical notes: Amir Hossein Yousefi received his PhD in Civil Engineering from University of Najafabad in 2020. He is currently Assistant Professor at the Department of Civil Engineering, shahinshahr University, Isfahan, Iran. **Farhad Kiani** received his PhD in Mechanical Engineering from University of Kashan in 2019. He is currently Assistant Professor at the Department of Mechanical Engineering, Shahinshahr University, Isfahan, Iran. **Esmaeil Abedi** is lecturer of Mechanical Engineering at the University of Kashan, Iran. His received her Mechanical Engineering from Shahid Bahonar Kerman University in 2004. His current research focuses on vibration, Rapid prototyping and control.

Research paper

1 INTRODUCTION

The use and application of Nano/Micro-Electro-Mechanical systems (NEMs/MEMs) are growing in various industries such as medicine, aerospace and biotechnology. In particular, microbeams are present in Atomic Force Microscope (AFM), micro-switches, micro-actuators, biosensors and micro-accelerometer by Ghayesh et al. [1] and Gomathi et al. [2]. Lightweight and resistance, and reduction of noise and vibrations in micro-electro-mechanical systems are important things which are always considered by the researchers. For example, due to thermal resistance in most of the sandwich microbeam, Functionally Graded Materials (FGM) have been used at different faces and viscoelastic materials are used in the core for better damping property. Functionally graded materials are a class of composites which change in their general mechanical properties is steadily from one surface to another. These materials are made of metal and ceramic which are produced by metallurgical powder and have no boundary problem in the layers. Form of materials distribution in matrix can be in form of power law (Λ, V, X) or exponential or uniform.

Nowadays, other compounds such as functionally graded carbon nanotube reinforced composite (FG-CNTRC) and boron nitride nanotube (BNNT) are used in the functionally graded materials as amplifiers instead of metal compound by Mohammadimehr and Alimirzaei. [3]. Smart materials such as Shape memory alloys by Asadi [4], piezoelectric or rheological materials are used to control vibrations in micro structures and due to the need for a low power source and low voltage, these systems are called semi-active. Rheological are materials which their general mechanical properties change, such as shear modulus, viscosity, and yield stress with electric field (ER materials) or magnetic field (MR materials). Various models have been proposed for the behavior of viscoelastic rheological materials, the most important of which are Complex modulus, Kelvin material model for pre-yield and Bingham plastic model for post-yield and Maxwell model by Yeh [5], El Wahed et al. [6]. Works done on macro and nano and microbeams with FGM faces and viscoelastic core are summarized as follows:

A) Studies and papers performed in macro size with classic theories: That includes analysis static of bending, buckling, free and forced vibration analysis, control and optimization vibrations. The natural frequency and the loss factor in viscoelastic materials such as electrorheological heavily depend on shear modulus. The real part is called the storage modulus and the imaginary part is called the loss modulus in complex modulus model. Yalcintas and Coulter [7] examined free vibrations of sandwich macro beam with the electrorheological core with different boundary conditions. They examined the effects of the electric field on a complex modulus and showed that lowering the constraints and supporting conditions will reduce natural frequency and increase loss factor. Arikoglu and Ozkol [8] investigated free vibrations of sandwich beam with composite faces and viscoelastic core using semi-analytic differential-transfer technique (DTM). They studied the effects of thickness, length, angles of fibers in the beam faces and different boundary conditions on natural frequency and the loss factor. Other model that is offered for viscoelastic/rheological materials in the pre-yield area is Kelvin model. Rahn and Joshi [9] used Kelvin material model to evaluate control of longitudinal vibrations of sandwich beam with ER core using Lyapunov Theory and Linear-Quadratic Regulator (LQR) method. Another model which is presented for rheological materials in the post-yield area is Bingham plastic model. Rezaeepazhand and Pahlavan [10] used Bingham plastic model to evaluate forced vibrations of sandwich beam with ER core. They used finite element method for spatial derivatives solvation and used central finite difference method for time derivatives solvation of partial differential Equations. Other methods for vibration analysis of sandwich beam are methods with mesh such as finite element and inverse method which were used by Adessina et al. [11] to evaluate forced vibrations of sandwich beam with viscoelastic core under dynamic load with different boundary conditions. Bhangale and Ganesan [12], conducted free vibration and static bending of sandwich microbeams with viscoelastic core under thermal load. Allahverdizadeh et al. [13] used Particle Swarm Optimization (PSO) algorithm for vibration analysis and optimization of sandwich beam with FGM faces and suggested amount of optimal volume fraction and optimal layer thickness. In addition, Allahverdizadeh et al. [14] investigated the natural frequency and loss factor for this sandwich beam. Different methods have been recommended for vibration control of sandwich beams in which intelligent materials are used as sensors and actuators. Modern control methods such as active feedback control and feedforward by Vasques and Rodrigues [15], Active Noise Control (ANC) and Active Vibration Control (AVC) [16], Hybrid active and passive control by Benjeddou [17], Adaptive control, Positive position Control [18], Independent Space Control [19], H2 / H∞ Optimized Control [20], linear Quadratic gaussian (LQR) [21] can also be mentioned.

B) Free and forced vibration analysis and vibration control of sandwich microbeam: Given that the classic theory of elasticity is not capable of predicting and expressing the behavior of systems in very small faces (nano and micro), different mathematical models are

proposed as non-classical elasticity theory. Experimental experiments to calculate the natural frequency and behavior of systems in very small faces are extremely costly and that is why these mathematical models have been used for the last two decades. The Nonlocal theory of elasticity by Eringen [22] can be considered to be among these models. Ebrahimi and Shafiei [23] used meshless General Differential Quadratic Method (GDQM) to evaluate free vibrations of Rotating Nano beam (FGM) using this theory. Shen et al. [24] evaluated forced vibrations of this nanobeam under dynamic load in a longitudinal and transverse direction. Evaluation of length parameter effects and changes of volume fraction indicator on sandwich microbeam with different boundary conditions using semi conductive differential transformation method (DTM) was done by Ebrahimi and Salari [25]. Other nonclassical theories such as surface elasticity by Gurtin et al. [26], micro polar theory [27] and couple stress theory which consists of four constant materials (two fixed numbers and two additional numbers) have also been presented [28]. Another important theory among these theories is the theory of strain gradient [29]. In this theory, high-order tensors such as deviation tensor and expansion tensor are considered and that is why Equations are wrapped and have higher length scale parameters. Ghorbanpour Arani et al. [30] used this theory to analyze the vibrations of sandwich microbeam using the DQM method of without Square Difference mesh. Also, Mohammadimehr and Monajemi [31] examined the buckling and free vibrations of FGM nanobeam reinforced with nitrite and boron. Yang et al. [32] presented the modified couplestress theory in which there is only need for expression of one length scale parameter. Density of Functional strain energy in modified couple stress theory was from square tensor of strain and symmetric part of the curvature tensor where length scale parameter only appeared in the curvature tensor. Şimşek and Reddy [33] examined the flexion and free vibrations of FTG sandwich microbeam using this theory and evaluated the effect of small length scale parameter on level of static deflection and natural frequency, they also evaluated the buckling phenomenon under critical load on microbeam with high order theories. The analysis of the forced vibrations of Timoshenko's sandwich nanobeam on Elastic base was done by Akbas [34]. Roque et al. [35] studied the optimal amount of volumetric fraction and thickness of layers in FGM sandwich microbeam.

In recent years. Different analytical and semi-analytical methods have been proposed for analyzing sandwich microbeams with FGM layers and Viscose core. Semi-analytic methods such as He,s Method [36], Rayleigh-Ritz Method [37], Arefi et al. [38] Combined methods with the use of Galerkin method, finite element methods were used by Asemi et al. [39] and mesh less methods such as GDQM by Ghorbanpour Arani et al. [40]. Basic Radial Functions (RBF) method is among suitable numerical methods used for complex forms. Convergence is possible with low number of points in this method due to lack of dependence of points to speed domain [41]. Other methods are combinations of two or more methods to reduce the defects of any of these methods such as combination of square differential method and base radial function method done by Shu et al. [42]. In this article, we have used base radial functions method to evaluate free vibrations of sandwich microbeam with FGM faces and viscoelastic/ER core. Then, combination of base radial functions method and leading finite difference method led to evaluation of forced vibrations of this sandwich microbeam with different boundary conditions. Then, we have used LQG control method to design and calculate suitable controller in the intended form for the intended system. Complex shear modulus model, Kelvin material model and Bingham plastic model have been considered in order to validate various models and comparison has been done with valid articles. In the end, we have evaluated the effect of length scale parameter (modified couple stress theory) and variation of the electric field on natural frequency and loss factor.

2 SYSTEM MODEL

2.1. Properties of ER Materials

Electrorheological is a substance with a behavior near to Newtonian fluids. Its mechanical properties shear modulus and viscosity change under the influence of electric field in a way that it turns into having an organized atomic structure and atomic arrangement in a regular manner. The electric field is indicated by E (KV/mm) and changes between 0 and 5. Increased electric field leads to behaviour of this material to become closer to the solid state. The point of yield in this diagram is extremely important and points before this point is called pre-yield and points after it are called post-yield. The stress and strain Equation for this substance is as follows:

$$\tau_{xz} = G^{*}\gamma, and G^{*} = G^{'} + G^{''}i \quad (1)$$

Where, τ_{xz} and γ are shear stress and strain and G* is the complex shear modulus which changes under the effect of electric field. In which G′ is storage modulus and G″ is loss factor. The different models are defined for viscoelastic materials in pre-yield area and plastic models in post-yield area. One of these models is Kelvin which is defined for pre-yield area. In this model, shear stress is modeled in parallel equal to a spring and a

damper. If G is stiffness of the spring and η is damping of a viscous damper, it can be written:

$$\tau_{xz} = \eta\dot{\gamma} + G\gamma, G(E) = m_g E + b_g, \eta(E) = m_e E + b_e \quad (2)$$

In which, $\dot{\gamma}$ is the rate of Shear strain variations. In which m_g, b_g, m_e and b_e are obtained in laboratory. Bingham plastic model is among other models in post-yield area, that τ_p and η_p are respectively shear stress and viscosity base coefficient for ER material post-yield area, it can be written as:

$$\tau_p(E) = \eta_p\dot{\gamma} + \tau_E(E), and \tau_E(E) = \alpha E^{\beta} \quad (3)$$

In which, τ_E is stress fluctuations which is a function of the electric field and the amount of η_p is separated from the electric field. In which α and β are the constants of ER material in the post-yield area and are determined in laboratory. All models are compared with valid article at the end of this study for validation.

2.2. Functionally Graded Materials (FGM)

Functionally graded materials are a combination of two different materials which are mostly made of ceramic and metal. This distribution non-homogeneously changes in line with thickness of the beam as shown in "Fig. 1".

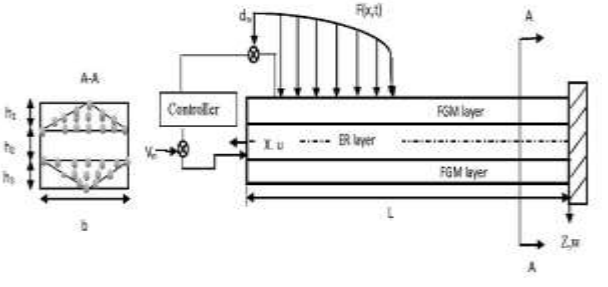

Fig. 1 A model of microbeam sandwich with ER core and FGMs faces.

Metal is distributed in power law form in layer one from top to bottom $(Z_1/2,-Z_1/2)$. This distribution is the opposite in the third layer $(Z_3/2,-Z_3/2)$. If the general mechanical properties of material for K[th] layer are shown with $P_k(Z)$, it can be written:

$$P_k(z) = P_T^{(k)} V_T^{(k)} + P_B^{(k)} V_B^{(k)} \quad (4)$$

In which P_B and P_T are general mechanical properties and V_B and V_T are volume fractions for highest and lowest levels of k[th] layer which can be expressed as follows:

$$V_T^1 = 1-(\frac{1}{2}-\frac{z_1}{h_1})^p \ , \ V_B^1 = (\frac{1}{2}-\frac{z_1}{h_1})^p$$
$$V_T^3 = (\frac{1}{2}+\frac{z_3}{h_3})^q \ , \ V_B^3 = 1-(\frac{1}{2}+\frac{z_3}{h_3})^q \quad (5)$$

p and q are related to volume fraction index for upper and lower microbeam layers.

2.3. Assumptions of the Problem

In this section, we will focus on displacement field and stress-strain relation based on the assumptions governing the problem. Assumptions governing the problem are as follows:

- ✓ The transverse deflection of beam is extremely small compared to thickness
- ✓ Core is made of viscoelastic materials (ER) and has shear deformation equal to the assumptions of Timoshenko beam
- ✓ Faces are made of FGM materials with power distribution and shear deformation in it has been ignored
- ✓ Layers do not slip on each other
- ✓ Transverse deformation is equal in all layers

If $u_k(x, y, z, t)$ and $w_k(x, y, z, t)$ are respectively the longitudinal and transversal deflections of k[th] layer of sandwich microbeam for any desired point, it can be written:

$$\begin{aligned}
u_1(x,z,t) &= u_0(x,t) - \frac{h_2}{2}\varphi(x,t) - \left(z+\frac{h_1}{2}\right)\frac{\partial w_1(x,t)}{\partial x} && -\frac{h_1}{2} \le z \le \frac{h_1}{2} \\
u_2(x,z,t) &= u_0(x,t) - z\varphi(x,t) && -\frac{h_2}{2} \le z \le \frac{h_2}{2} \\
u_3(x,z,t) &= u_0(x,t) + \frac{h_2}{2}\varphi(x,t) - \left(z-\frac{h_3}{2}\right)\frac{\partial w_3(x,t)}{\partial x} && -\frac{h_3}{2} \le z \le \frac{h_3}{2} \\
w_k(x,z,t) &= w(x,t) && i=1,2,3 \quad -\frac{h}{2} \le z \le \frac{h}{2}
\end{aligned} \quad (6)$$

In which, $u_0(x, t)$ and $w(x, t)$ are longitudinal and transverse deflection of the middle face of viscoelastic core. $\varphi(x,t)$ is the total change of core angles based on Timoshenko theory. It can be written based on displacement field Equation and von Kármán Equation:

$$\varepsilon_{xx}^{(1)} = \frac{\partial u_0}{\partial x} - \frac{h_2}{2}\frac{\partial \varphi}{\partial x} - \left(z+\frac{h_1}{2}\right)\frac{\partial^2 w}{\partial x^2}$$
$$\gamma_{xz}^{(2)} = \frac{\partial w}{\partial x} - \varphi \quad (7)$$
$$\varepsilon_{xx}^{(3)} = \frac{\partial u_0}{\partial x} + \frac{h_2}{2}\frac{\partial \varphi}{\partial x} - \left(z-\frac{h_3}{2}\right)\frac{\partial^2 w}{\partial x^2}$$

In which, ε is the longitudinal strains in upper and lower faces and γ is the shear strain in core. It can be written according to Hooke's Equation that:

$$\sigma_{xx}^{(1)} = E_1(z)\varepsilon_{xx}^{(1)} \ , \ \sigma_{xz}^{(2)} = G_2^* \gamma_{xz}^{(2)} \ , \ \sigma_{xx}^{(3)} = E_3(z)\varepsilon_{xx}^{(3)} \qquad (8)$$

In which, $E_1(z)$ and $E_3(z)$ are Young's modulus for upper and lower faces in functionally graded materials and G_2^* is complex shear modulus for Viscoelastic core of ER according to "Eqs. (4-5)".

2.4. Modified Couple Stress Theory

In this section, we will use modified couple stress theory expressed by Young et al. (2002) for materials in micro-size to extract strain energy Equations. According to this theory, the energy of strain potential includes two sections of square tensor of the strain and curvature tensor (which only includes length scale parameter). In this theory, the density of strain energy of u for sandwich microbeam with infinite shape transformation is as follows:

$$U = \frac{1}{2}\sum_{k=1}^{3}\iiint_V (\sigma_{ij}^k \varepsilon_{ij}^k + m_{ij}^k \chi_{ij}^k) dV \qquad (9)$$

In which σ and ε are symmetric parts of stress and strain tensor and χ and m are respectively symmetric part of curvature tensor and deviatory part of coupled stress tensor.

$$\begin{aligned} \chi_{ij}^k &= \frac{1}{2}\left[(\nabla\theta)_{ij}^k + ((\nabla\theta)_{ij}^k)^T\right] \\ m_{ij}^k &= 2l_k^2 \mu^k \chi_{ij}^k \end{aligned} \qquad (10)$$

The infinitesimal rotary vector generated by the deflection field is also defined as follows:

$$\theta_i^k = \frac{1}{2}(curl\,(u))_i^k \qquad (11)$$

In which l is length scale parameter which applies the effects of size in curvature tensor. Also, the amount of $\mu^{(k)}$ is the Shear stress for k[th] layer.

3 GOVERNING EQUATIONS

According to Hamilton's principle, the motion Equation for sandwich microbeam under external load and electric field is as follows:

$$\int_{t_1}^{t_2} (\delta T - \delta U + \delta W_{ext} + \delta W_{er})\, dt = 0 \qquad (12)$$

In which, T is the Kinetic energy of the system, U is the strain energy and W_{ext} is work resulting from outside forces and W_{er} is the virtual work caused by electric field changes in ER, and δ is related to variation operator. It can be written by applying variation in "Eq. (9)" for strain energy:

$$\delta U = b\int_0^L \left\{ \begin{array}{l} \left[N_{xx}^{(1)}\left(\frac{\partial \delta u_0}{\partial x} - \frac{h_2}{2}\frac{\partial \delta\varphi}{\partial x} - \frac{h_1}{2}\frac{\partial^2 \delta w}{\partial x^2}\right) - M_{xx}^{(1)}\frac{\partial^2 \delta w}{\partial x^2}\right] \\ +Q_{xz}^{(2)}\left(\frac{\partial \delta w}{\partial x} - \delta\varphi\right) \\ +\left[N_{xx}^{(3)}\left(\frac{\partial \delta u_0}{\partial x} + \frac{h_2}{2}\frac{\partial \delta\varphi}{\partial x} + \frac{h_3}{2}\frac{\partial^2 \delta w}{\partial x^2}\right) - M_{xx}^{(3)}\frac{\partial^2 \delta w}{\partial x^2}\right] \\ -\frac{1}{2}S_{xy}^{(1)}\frac{\partial^2 \delta w}{\partial x^2} - \frac{1}{2}S_{xy}^{(3)}\frac{\partial^2 \delta w}{\partial x^2} - \frac{1}{4}S_{xy}^{(2)}\left(\frac{\partial \delta\varphi}{\partial x} + \frac{\partial^2 \delta w}{\partial x^2}\right) \end{array} \right\} dx \qquad (13)$$

The values of N, M, Q are respectively normal new axial, flexural, and shear and S forces related to modified couple in k[th] layer and are defined as follows:

$$(N_{xx}^{(k)}, M_{xx}^{(k)}, S_{xy}^{(k)}) = \int_{-\frac{h_k}{2}}^{\frac{h_k}{2}} (\sigma_{xx}^{(k)}, z\sigma_{xx}^{(k)}, m_{xy}^{(k)})\, dz \quad , \quad Q_{xz}^{(2)} = \int_{-\frac{h_2}{2}}^{\frac{h_2}{2}} \sigma_{xz}^{(2)} dz \qquad (14)$$

By substituting "Eq. (14) into Eq. (13)", we can obtain the following Equation:

$$\delta U = b\int_0^L \left(N\frac{\partial \delta u_0}{\partial x} - R\frac{\partial \delta\varphi}{\partial x} - M\frac{\partial^2 \delta w}{\partial x^2} + Q_{xz}^{(2)}\frac{\partial \delta w}{\partial x} - Q_{xz}^{(2)}\delta\varphi \right) dx \qquad (15)$$

Which can be written for the coefficients N, M, R:

$$\begin{aligned}
N &= N_{xx}^{(1)} + N_{xx}^{(3)} = A_{11}\frac{\partial u_0}{\partial x} - A_{12}\frac{\partial \varphi}{\partial x} - A_{13}\frac{\partial^2 w}{\partial x^2} \\
R &= \left(N_{xx}^{(1)} - N_{xx}^{(3)}\right)\frac{h_2}{2} + \frac{S_{xy}^{(2)}}{4} \\
&= A_{21}\frac{\partial u_0}{\partial x} - A_{22}\frac{\partial \varphi}{\partial x} - A_{23}\frac{\partial^2 w}{\partial x^2} \\
M &= M_{xx}^{(1)} + M_{xx}^{(3)} + \frac{1}{2}\left(N_{xx}^{(1)}h_1 - N_{xx}^{(3)}h_3\right) + \frac{S_{xy}^{(1)}}{2} \\
&\quad + \frac{S_{xy}^{(3)}}{2} + \frac{S_{xy}^{(2)}}{4} \\
&= A_{31}\frac{\partial u_0}{\partial x} - A_{32}\frac{\partial \varphi}{\partial x} - A_{33}\frac{\partial^2 w}{\partial x^2}
\end{aligned} \tag{16}$$

The coefficients of the deflection variables in "Eq. (16)" which are A_{ij} form a symmetric matrix equal to:

$$\begin{aligned}
A_{11} &= E_m(h_1 + h_3) + (E_c - E_m)\left(\frac{h_1}{p+1} + \frac{h_3}{q+1}\right) \\
A_{12} &= \left[E_m(h_1 - h_3) + (E_c - E_m)\left(\frac{h_1}{p+1} - \frac{h_3}{q+1}\right)\right]\frac{h_2}{2} \\
A_{13} &= \frac{E_m}{2}(h_1^2 - h_3^2) + (E_c - E_m)\left(\frac{h_1^2}{p+2} - \frac{h_3^2}{q+2}\right) \\
A_{21} &= A_{12} \\
A_{22} &= \left[E_m(h_1 + h_3)\frac{h_2^2}{4} + (E_c - E_m)\left(\frac{h_1}{p+1} + \frac{h_3}{q+1}\right)\frac{h_2^2}{4} + G_2^* l_2^2\frac{h_2}{8}\right] \\
A_{23} &= \left[\frac{E_m}{2}(h_1^2 + h_3^2) + (E_c - E_m)\left(\frac{h_1^2}{p+2} + \frac{h_3^2}{q+2}\right) + \frac{G_2^* l_2^2}{4}\right]\frac{h_2}{2} \\
A_{31} &= A_{13} \\
A_{32} &= A_{23} \\
A_{33} &= \frac{E_m}{3}(h_1^3 + h_3^3) + (E_c - E_m)\left(\frac{h_1^3}{p+3} + \frac{h_3^3}{q+2}\right) + \\
&\frac{G_m}{2}(h_1 l_1^2 + h_3 l_3^2) + \frac{(G_c - G_m)}{2}\left(\frac{h_1 l_1^2}{p+1} + \frac{h_3 l_3^2}{q+1}\right) + \frac{G_2^* h_2 l_2^2}{8}
\end{aligned} \tag{17}$$

In "Eq. (17)", only the A_{22}, A_{23}, A_{32} *and* A_{33} strings have a length scale parameter that shows curvature tensor. The kinetic energy for a sandwich microbeam can be expressed as follows:

$$T = \frac{1}{2}\sum_{k=1}^{3}\iiint_V \rho(\dot{U}_k)^2\, dV \tag{18}$$

In which ρ_k is the density and $\dot{U}$ is the speed at any desired point of microbeam and moment of inertia in k[th] layer can be written as:

$$I_0^{(k)}, I_1^{(k)}, I_2^{(k)} = \int_{-\frac{h_k}{2}}^{\frac{h_k}{2}} (1, z, z^2)\rho_k(z)\, dz \tag{19}$$

With the factorial of the displacement coefficients in "Eq. (18)", the inertia related terms in "Eq. (19)" are defined as:

$$\begin{aligned}
I_0 &= I_0^{(1)} + I_0^{(3)} + I_0^{(2)} \\
I_1 &= I_2^{(2)} + \left(I_0^{(1)} + I_0^{(3)}\right)\frac{h_2^2}{4} \\
I_2 &= \left(I_0^{(1)} - I_0^{(3)}\right)h_2 \\
I_3 &= 2I_1^{(1)} + 2I_1^{(3)} + I_0^{(1)}h_1 - I_0^{(3)}h_3 \\
I_4 &= \left(2I_1^{(1)} - 2I_1^{(3)} + I_0^{(1)}h_1 + I_0^{(3)}h_3\right)\frac{h_2}{2} \\
I_5 &= I_2^{(1)} + I_2^{(3)} + I_1^{(1)}h_1 - I_1^{(3)}h_3 + \frac{1}{4}\left(I_0^{(1)}h_1^2 + I_0^{(3)}h_3^2\right)
\end{aligned} \tag{20}$$

The variation of kinetic energy in "Eq. (18)" can be written as:

$$\delta T = \frac{b}{2}\int_0^L \left[\begin{aligned}
&I_0\delta\dot{u}_0^2 + I_0\delta\dot{w}^2 + I_1\delta\dot{\varphi}^2 - I_2\delta\left(\dot{u}_0\dot{\varphi}\right) \\
&-I_3\delta\left(\dot{u}_0\frac{\partial\dot{w}}{\partial x}\right) + I_4\delta\left(\dot{\varphi}\frac{\partial\dot{w}}{\partial x}\right) + I_5\delta\left(\frac{\partial\dot{w}}{\partial x}\right)^2
\end{aligned}\right] dx \tag{21}$$

If the loading of width on microbeam is shown with $F(x,t)$, virtual work caused by external force is equal to:

$$\delta W_{ext} = \int_V F_{ext}\delta w\, dV \tag{22}$$

And also, virtual work caused by changes on electric field in electrorheological core is as follows:

$$\delta W_{er} = -\eta\int_V \dot{\gamma}\delta\gamma\, dV \tag{23}$$

"Eq. (23)" changes based on consideration of proper model for electrorheological core which will be discussed at validation of forced vibrations. The general motion Equation governing the sandwich microbeam is obtained as follows:

$$\begin{aligned}
&\delta u_0:\ A_{11}\frac{\partial^2 u_0}{\partial x^2}-A_{12}\frac{\partial^2 \varphi}{\partial x^2}-A_{13}\frac{\partial^3 w}{\partial x^3}-I_0\ddot{u}_0+\frac{1}{2}I_2\ddot{\varphi}+\frac{1}{2}I_3\frac{\partial \ddot{w}}{\partial x}=0\\
&\delta\varphi:\ -A_{21}\frac{\partial^2 u_0}{\partial x^2}+A_{22}\frac{\partial^2 \varphi}{\partial x^2}-G_2^* h_2\varphi+A_{23}\frac{\partial^3 w}{\partial x^3}+G_2^* h_2\frac{\partial w}{\partial x}+\\
&\quad\frac{1}{2}I_2\ddot{u}_0-I_1\ddot{\varphi}-\frac{1}{2}I_4\frac{\partial \ddot{w}}{\partial x}+F_{er}^{\varphi}=0\\
&\delta w:\ A_{31}\frac{\partial^3 u_0}{\partial x^3}-A_{32}\frac{\partial^3 \varphi}{\partial x^3}-G_2^* h_2\frac{\partial \varphi}{\partial x}-A_{33}\frac{\partial^4 w}{\partial x^4}+G_2^* h_2\frac{\partial^2 w}{\partial x^2}-\\
&\quad\frac{1}{2}I_3\frac{\partial \ddot{u}_0}{\partial x}+\frac{1}{2}I_4\frac{\partial \ddot{\varphi}}{\partial x}+I_5\frac{\partial^2 \ddot{w}}{\partial x^2}-I_0\ddot{w}+F_{er}^{w}=F_{ext}
\end{aligned} \tag{24}$$

Also, the remaining terms outside the integral in "Eq. (12)" represent boundary conditions and can be written as:

$$\begin{aligned}
&N\,\delta u_0=0\\
&R\,\delta\varphi=0\\
&\left(Q_{xz}^{(2)}+\frac{\partial M}{\partial x}-\frac{1}{2}I_3\ddot{u}_0+\frac{1}{2}I_4\ddot{\varphi}+I_5\frac{\partial \ddot{w}}{\partial x}\right)\delta w=0\\
&M\,\delta\left(\frac{\partial w}{\partial x}\right)=0
\end{aligned} \tag{25}$$

The matrix form of "Eq. (24)" for free vibrations, can be written as follows:

$$[K]\{\alpha\}=\omega_m^2[M]\{\alpha\} \tag{26}$$

Where, [M] and [K] are the matrix of mass and Stiffness and α is the eigenvector of displacement. In the method of radial basis function (RBF), we separate vector of deflection *(V_s)* to time and space functions described in section (4), with assumption of harmonic movement can be written as:

$$V_s=\begin{Bmatrix}u_0(\mathrm{x})\\ \varphi(\mathrm{x})\\ w(\mathrm{x})\end{Bmatrix}=\begin{Bmatrix}\sum_{j=1}^{N}\alpha_j^{u_0}g_j(\|x-x_j\|,\mathrm{c})e^{i\omega_m t}\\ \sum_{j=1}^{N}\alpha_j^{\varphi}g_j(\|x-x_j\|,\mathrm{c})e^{i\omega_m t}\\ \sum_{j=1}^{N}\alpha_j^{w}g_j(\|x-x_j\|,\mathrm{c})e^{i\omega_m t}\end{Bmatrix} \tag{27}$$

In which ω_m is the complex radian frequency (rad/s) and α is weight coefficients and can be distinguished as follows:

$$\omega_m^2=\Omega^2(1+\xi i) \tag{28}$$

In which Ω is the Natural frequency and ξ is loss factor and is equal to:

$$\Omega=\sqrt{\mathrm{Re}(\omega_m^2)}\quad,\quad \xi=\frac{\mathrm{Im}(\omega_m^2)}{\mathrm{Re}(\omega_m^2)} \tag{29}$$

4 RBF NUMERICAL METHOD FOR CALCULATING FREE VIBRATION

One of the mesh less numerical methods is radial base functions (RBFs). This method is suitable for complex forms and has a high convergence due to the lack of dependence of the distribution of points to the domain. In a way that the general form of a differential Equation is as follows:

$$\begin{aligned}
&Lu(x)=\omega_m^2 u(x)\ \ in\quad \psi\\
&Bu(x)=0\qquad on\quad \partial\psi
\end{aligned} \tag{30}$$

In which L is the linear differential operator on Ψ domain and B is the linear differential operator on $\partial\Psi$ boundaries and with assumption distribution of N_s points on each layer of sandwich microbeam, in general we will have *3Ns*3Ns* matrices of domain and boundaries. Distribution of points in accordance with Gauss-Chebyshev-Lobatto is as follows:

$$x_i=\frac{L}{2}\left\{1-\cos\left[\frac{(i-1)\pi}{(N-1)}\right]\right\},\ (i=1,2,3,\ldots,N) \tag{31}$$

According to having four boundary conditions for each side of sandwich microbeam, the following nodes can be considered as boundaries:

$$\{1,N,N+1,2N,2N+1,2N+2,3N-1,3N\}\in\psi \tag{32}$$

There are different models to express radial base function in RBF method, the most important of which are:

$$\begin{aligned}
&g=r^{2c}Log(r) && thin\ plate\ spline\\
&g=e^{-c^2 r} && Gaussian\ function\\
&g=r^2 && Polynomial\ function\\
&g=(r^2+c^2)^{(1/2)} && Multiquadric\ function\\
&g=(r^2+c^2)^{(-1/2)} && Inverse\ Multiquadric\ function\\
&and\ \ r=\|X-X_j\|=\sqrt{(x-x_j)^2+(y-y_j)^2}
\end{aligned} \tag{33}$$

Several multiqaudrat functions have been used in this article in which c is the parameter of shape. Selection of parameter c is extremely important for obtaining the correct answer. The optimal value after the guess and error is about $c= 1.7 (Ns)^{-0.5}$ and *Ns* is the number of points on one layer of the beam. The following general form is obtained for the differential Equation system by placing "Eq. (33)" in "Eq. (30)":

$$\sum_{j=1}^{N} \alpha_j Lg(\|X_i - X_j\|, c) = \omega_m^2 \sum_{j=1}^{N} \alpha_j Lg(\|X_i - X_j\|, c), i \in \psi \quad (34)$$
$$\sum_{j=1}^{N} \alpha_j Bg(\|X_i - X_j\|, c) = 0, i \in \psi$$

The matrix form of "Eq. (34)" is as follows:

$$\begin{bmatrix} Lg \\ Bg \end{bmatrix} \{\alpha\} = \omega_m^2 \begin{bmatrix} g \\ 0 \end{bmatrix} \{\alpha\} \quad (35)$$

In which ω_m is the eigenvalue. It can be written by placing "Eq. (27)" in "Eq. (24)":

$$\sum_{j=1}^{N} \alpha_j^{u_0} (A_{11} \frac{\partial^2 g}{\partial x^2}) - \sum_{j=1}^{N} \alpha_j^{\varphi} (A_{12} \frac{\partial^2 g}{\partial x^2}) - \sum_{j=1}^{N} \alpha_j^{w} (A_{13} \frac{\partial^3 g}{\partial x^3}) =$$
$$\omega_m^2 \left(\sum_{j=1}^{N} \alpha_j^{u_0} (I_0 g) - \frac{1}{2} \sum_{j=1}^{N} \alpha_j^{\varphi} (I_2 g) - \frac{1}{2} \sum_{j=1}^{N} \alpha_j^{w} (I_3 \frac{\partial g}{\partial x}) \right)$$
$$- \sum_{j=1}^{N} \alpha_j^{u_0} (A_{21} \frac{\partial^2 g}{\partial x^2}) + \sum_{j=1}^{N} \alpha_j^{\varphi} (A_{22} \frac{\partial^2 g}{\partial x^2}) - \sum_{j=1}^{N} \alpha_j^{\varphi} (G_2 h_2 g) +$$
$$\sum_{j=1}^{N} \alpha_j^{w} (A_{23} \frac{\partial^3 g}{\partial x^3}) + \sum_{j=1}^{N} \alpha_j^{w} (G_2 h_2 \frac{\partial g}{\partial x}) =$$
$$\omega_m^2 \left(\frac{1}{2} \sum_{j=1}^{N} \alpha_j^{u_0} (I_2 g) + \sum_{j=1}^{N} \alpha_j^{\varphi} (I_1 g) + \frac{1}{2} \sum_{j=1}^{N} \alpha_j^{w} (I_4 \frac{\partial g}{\partial x}) \right) \quad (36)$$
$$\sum_{j=1}^{N} \alpha_j^{u_0} (A_{31} \frac{\partial^3 g}{\partial x^3}) - \sum_{j=1}^{N} \alpha_j^{\varphi} (A_{32} \frac{\partial^3 g}{\partial x^3}) - \sum_{j=1}^{N} \alpha_j^{\varphi} (G_2 h_2 \frac{\partial g}{\partial x}) - \sum_{j=1}^{N} \alpha_j^{w} (A_{33} \frac{\partial^2 g}{\partial x^2}) +$$
$$\sum_{j=1}^{N} \alpha_j^{w} (G_2 h_2 \frac{\partial^2 g}{\partial x^2}) = \omega_m^2 \begin{pmatrix} \frac{1}{2} \sum_{j=1}^{N} \alpha_j^{u_0} (I_3 \frac{\partial g}{\partial x}) - \frac{1}{2} \sum_{j=1}^{N} \alpha_j^{\varphi} (I_4 \frac{\partial g}{\partial x}) - \\ \frac{1}{2} \sum_{j=1}^{N} \alpha_j^{w} (I_5 \frac{\partial^2 g}{\partial x^2}) + \sum_{j=1}^{N} \alpha_j^{w} (I_0 g) \end{pmatrix}$$

Then, the natural frequency and loss factor are obtained using "Eq. (28)".

5 FORCED VIBRATIONS

The transverse force of *F(x, t)* and the force of F_{er} obtained from changing electric field are applied to the ER core. There are different models for changing electric field of the ER core. We have used complex shear modulus models as well as Kelvin material model in the pre-yield area and Bingham model in the post-yield area in examples mentioned in this article and these have been validated with credible articles. Solvation of differential Equations based on time is done in this method by dividing time steps to Δt using Forward difference rule method and Nicholson-Crank's assumptions. The general form of sandwich microbeam's motion Equation by combining the leading differential and RBF method is as follows:

$$A_{11} \frac{u_{0xx}^{n+1} + u_{0xx}^{n}}{2} - A_{12} \frac{\varphi_{xx}^{n+1} + \varphi_{xx}^{n}}{2} - A_{13} \frac{w_{xxx}^{n+1} + w_{xxx}^{n}}{2} -$$
$$I_0 \frac{u_0^{n+1} - 2u_0^{n} + u_0^{n-1}}{(\Delta t)^2} + \frac{1}{2} I_2 \frac{\varphi^{n+1} - 2\varphi^{n} + \varphi^{n-1}}{(\Delta t)^2} +$$
$$\frac{1}{2} I_3 \frac{w_x^{n+1} - 2w_x^{n} + w_x^{n-1}}{(\Delta t)^2} = 0$$
$$-A_{21} \frac{u_{0xx}^{n+1} + u_{0xx}^{n}}{2} + A_{22} \frac{\varphi_{xx}^{n+1} + \varphi_{xx}^{n}}{2} - G_2^* h_2 \frac{\varphi^{n+1} + \varphi^{n}}{2} +$$
$$A_{23} \frac{w_{xxx}^{n+1} + w_{xxx}^{n}}{2} + G_2^* h_2 \frac{w_x^{n+1} + w_x^{n}}{2} + \frac{1}{2} I_2 \frac{u_0^{n+1} - 2u_0^{n} + u_0^{n-1}}{(\Delta t)^2} -$$
$$I_1 \frac{\varphi^{n+1} - 2\varphi^{n} + \varphi^{n-1}}{(\Delta t)^2} - \frac{1}{2} I_4 \frac{w_x^{n+1} - 2w_x^{n} + w_x^{n-1}}{(\Delta t)^2} + F_{er}^{\varphi} = 0$$
$$-A_{21} \frac{u_{0xx}^{n+1} + u_{0xx}^{n}}{2} + A_{22} \frac{\varphi_{xx}^{n+1} + \varphi_{xx}^{n}}{2} - G_2^* h_2 \frac{\varphi^{n+1} + \varphi^{n}}{2} + \quad (37)$$
$$A_{23} \frac{w_{xxx}^{n+1} + w_{xxx}^{n}}{2} + G_2^* h_2 \frac{w_x^{n+1} + w_x^{n}}{2} + \frac{1}{2} I_2 \frac{u_0^{n+1} - 2u_0^{n} + u_0^{n-1}}{(\Delta t)^2} -$$
$$I_1 \frac{\varphi^{n+1} - 2\varphi^{n} + \varphi^{n-1}}{(\Delta t)^2} - \frac{1}{2} I_4 \frac{w_x^{n+1} - 2w_x^{n} + w_x^{n-1}}{(\Delta t)^2} + F_{er}^{\varphi} = 0$$
$$A_{31} \frac{u_{0xxx}^{n+1} + u_{0xxx}^{n}}{2} - A_{32} \frac{\varphi_{xxx}^{n+1} + \varphi_{xxx}^{n}}{2} - G_2^* h_2 \frac{\varphi_x^{n+1} + \varphi_x^{n}}{2} -$$
$$A_{33} \frac{w_{xxxx}^{n+1} + w_{xxxx}^{n}}{2} + G_2^* h_2 \frac{w_{xx}^{n+1} + w_{xx}^{n}}{2} - \frac{1}{2} I_3 \frac{u_{0x}^{n+1} - 2u_{0x}^{n} + u_{0x}^{n-1}}{(\Delta t)^2} +$$
$$\frac{1}{2} I_4 \frac{\varphi_x^{n+1} - 2\varphi_x^{n} + \varphi_x^{n-1}}{(\Delta t)^2} + I_5 \frac{w_{xx}^{n+1} - 2w_{xx}^{n} + w_{xx}^{n-1}}{(\Delta t)^2} -$$
$$I_0 \frac{w^{n+1} - 2w^{n} + w^{n-1}}{(\Delta t)^2} + F_{er}^{w} = F_{ext}$$

Based on the conditions of the problem at t_0 for Δt time step, time at the n^{th} moment can be defined in form of $t_n = t_0 + n\Delta t$ and we can move to $n + 1$ step. As can be seen, next step of $n-1$ steps which is n can be obtained from it. Location derivatives are calculated from RBF

and time derivatives are calculated from Forward difference rule method.

6 LQG CONTROLLER (REDUCED-ORDER MODAL)

V_{si} is the mode of displacements to i[th] mode, it can be written based on modal sum method to following form:

$$V_{si}(x,t)=\sum_{i=1}^{r} g_i(x)q_i(t) \tag{38}$$

Assuming proportional damping, and substituting "Eq. (38)" into "Eq. (24)", it can be written in the following form:

$$M\ddot{q}(t)+C\dot{q}(t)+Kq(t)+F_{er}=F_{ext} \tag{39}$$

The second order system above may be transformed to the following state space one:

$$\begin{aligned}&\{\dot{x}\}=[A]\{x\}+[B]\{z\}+\{f\},\\&\{y\}=[C]\{x\}\end{aligned} \tag{40}$$

Where each column of the control input matrix B represents the ER actuation loads distribution for a unitary electrical field and the control input z is a column vector formed by the electrical field E applied to the actuators. The perturbation vector *f* is the state distribution of the mechanical loads F_{ext} and the output vector y is, generally, composed of the measured quantities, written in terms of the state vector x through the output matrix C. The system dynamics are determined by the square matrix A. In "Eq. (24)", the generalized excitation force vector {f} and the matrix $[K_g]$ define the inputs, while {y} is the output vector. In the closed-loop configuration, the control input vector {z} in "Eq. (40)" is related to the state feedback vector, as:

$$\{z\}=-\left[K_g\right]\{x\},\ \{x\}=\left\{q_1\ \dot{q}_1.....q_n\ \dot{q}_n\right\}^T \tag{41}$$

The vector of mechanical and electrical force is as follows:

$$\{f\}=\left[\bar{M}^{-1}\bar{F}_{ext}\right],\ B=\left[\bar{M}^{-1}\bar{F}_{er}\right] \tag{42}$$

The feedback gain matrix is obtained so as to minimize the quadratic cost function of the form:

$$J=\frac{1}{2}\int_0^{\infty}(\{x\}^T[Q]\{x\}+\{z\}^T[R]\{z\})dt \tag{43}$$

Where, Q and R are the state variable and control input weighting matrices. $\{z\}= -[K_g]\{x\}$, where the control gain matrix, $[K_g]=[R]^{-1}[B]^T[P]$ is evaluated by solving [P] from the following algebraic Ricatti Equation:

$$A^T p+pA-PBR^{-1}B^T p+Q=0 \tag{44}$$

To estimate the states of the system from sensor outputs, an state estimator based on the Kalman filter is designed:

$$\dot{\hat{x}}=(A+BK_g)\hat{x}+f+k_e(y-C\hat{x}) \tag{45}$$

Where, x is the estimated state vector and K_e is the observer gain matrix. The Luenberger observer simulates real system and penalizes the difference between the measured output y and the estimated output Cx, Input d_w and output V_n noise contributions are added, respectively, to state excitation p and output measurement y in Equation (40). Hence, replacing $y=Cx+V_n$ in Equation (45), then subtracting the resulting Equation from the state space system, with added noise term d_w, leads to:

$$\dot{e}=(A-k_e c)e+d_w-k_e V_n \tag{46}$$

The optimal gain K*e* is then defined as:

$$k_e=pC^T V^{-1} \tag{47}$$

Combining the steady-state Kalman–Bucy filter with the steady-state LQR, the inter-related dynamic system will take the following form:

$$\begin{Bmatrix}\dot{x}\\ \dot{e}\end{Bmatrix}=\begin{bmatrix}A-BK_g & BK_g\\ 0 & A-K_eC\end{bmatrix}\begin{Bmatrix}x\\ e\end{Bmatrix}+\begin{bmatrix}I & 0\\ I & K_e\end{bmatrix}\begin{Bmatrix}d_w\\ V_n\end{Bmatrix}+\begin{Bmatrix}f\\ 0\end{Bmatrix} \tag{48}$$

Where, *e(t)* is the error between the true and estimated states and d_w and V_n are the plant and measurement noise vectors. The plant and measurement noise are both assumed to be white, and have a gaussian probability density function and are assumed uncorrelated with the inputs. Equations (44) and (47) are Lyapunov Equations and can be solved simultaneously using MATLAB software to determine the feedback gain.

7 VALIDATIONS OF MODELS

7.1. Sandwich Microbeam (Complex Shear Modulus)

In the first case, we study free sandwich microbeam vibrations made of functionally graded materials faces and viscoelastic core. In this

model, volume fractional index has been considered to be same in upper and lower layers [43]. The mechanical properties of the sandwich beam are in accordance with "Table 1".

Table 1 Material properties and dimensions

FGM layers
E_m=70 Gpa , E_c=472 Gpa
ν_m=0.3 , ν_c=0.17
ρ_m=2702 Kg/m^3 , ρ_c=3100 Kg/m^3
l_1=l_3=5 μm
Viscoelastic layer
G_2=4 Mpa
η=0.38
ρ_2=2000 Kg/m^3
l_2=7.5 μm

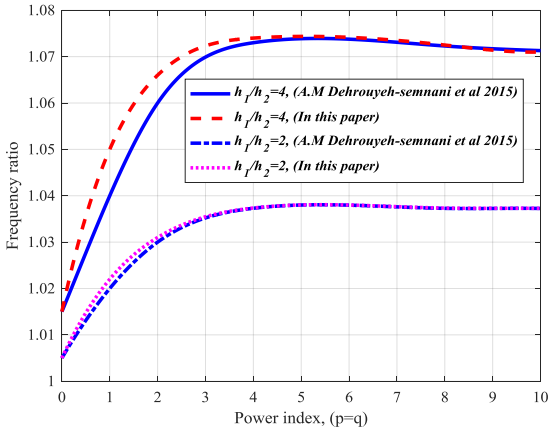

Fig. 3 Variation of the loss factor ratios (ξ) with the volume fractions index for h_2=l_2 and S-S microbeam.

As it can be observed in "Table 1", it has a low level of natural frequency and loss factor. Also, the ratio of natural frequency and loss factor are defined as follows:

$$\Omega_{\dim ensionless}=\frac{\Omega_{nonclassic}}{\Omega_{classic}},\ \xi_{\dim ensionless}=\frac{\xi_{nonclassic}}{\xi_{classic}} \quad (49)$$

There is a comparison between the article of Dehriouyeh-Semnani et al. [43] on the ratio of natural frequency and loss factor. There is comparison between frequency ratio and loss factor in "Figs. 2-3".

7.2. Kelvin Model

We apply the force off on it in order to study deformation of the end point of the tip of C-C beam. As it can be observed from "Fig. 4a", the first natural frequency Ω_1 decreases by increasing power index p and q at lower values of power index, but the first natural frequency tends to an approximately constant value as power index increases. In addition, the plotted results demonstrate that by increasing the value of length scale parameter l, the first natural frequency Ω_1 increases. It can be observed from "Fig. 4b", by increasing power index p and q, the first loss factor ξ_1 increases and then is approximately constant and also by increasing the value of length scale parameter l, the first loss factor ξ_1 decreases. Figure 5a illustrates that the first natural frequency decreases Ω_1 by increasing length of microbeam L at lower values of length microbeam, but it converges to a constant value by increasing length of microbeam. It can be observed from "Fig. 5b", by increasing length of microbeam L, the first loss factor ξ_1 increases and then decreases.

It can be seen from "Fig. 6a-b" that the first natural frequency Ω_1 and the first loss factor ξ_1 have ascending trends, respectively, with respect to electric field (E). Since with the increase of the electric field, the state of material ER to the solid is almost approaching, and the matrix of stiffness and damping increases, for this reason simultaneously the first natural frequency and first loss factor magnitude increase. In "Figs. 7a-8a", the first natural frequency decreases with increasing core thickness (h_2) and upper face thickness (h_1) as a result of the decreasing ratio of the sectional stiffness to mass. As shown in "Fig 7b", by increasing the core thickness of ER, the loss factor increases because the average material loss factor of the microbeam increases. In "Fig. 8b", by increasing the thickness of the upper layer, the amount of the loss factor first increased and then reduced because the system loss factor depends on both the material loss factor and stored strain energy. As the thickness of the FGM layers increases, the average material loss factor of the microbeam increases, however, the average strain energy stored by the faces due to the shear stress decreases. Therefore, the loss factors of the microbeam do not always increase with the faces thickness. Instead, an increase to a global maximum and then a decrease is observed.

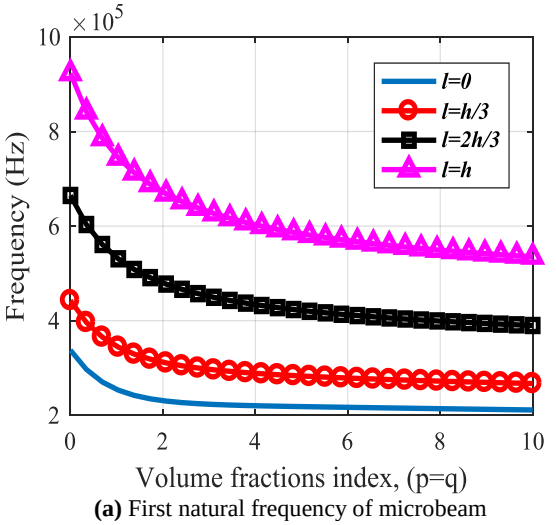

(a) First natural frequency of microbeam

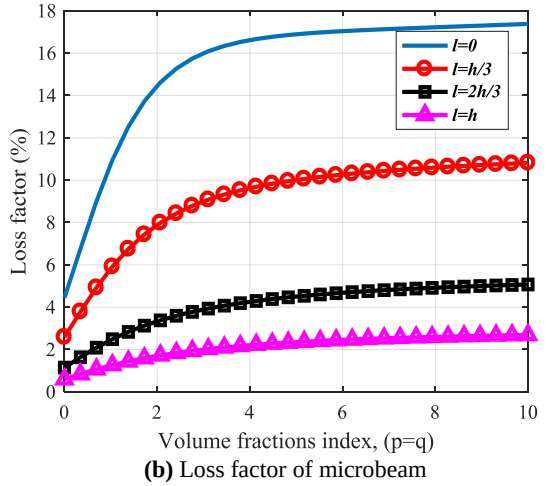

(b) Loss factor of microbeam

Fig. 4 Variation of the natural frequency and loss factor with the volume fractions index for E=1(KV/mm) and for various values of the dimensionless length scale parameter.

In "Fig. 9", we examine the different boundary conditions on the first natural frequency and the first loss factor. As it is known, with increased constraints of microbeam, the natural frequency increases and the loss factor of the system decreases. As the stiffness matrix increases, the shear stress decreases and the energy stored in the system decreases. In "Fig. 10", the three-dimensional diagram of the changes of the length scale parameter and electric field is plotted in terms of the first natural frequency and the loss factor for C-S boundary condition.

According to this diagram, the highest natural frequency is related to the maximum value of the electric field and of the length scale parameter, but the highest amount of loss factor is related to the greater electric field and the smallest of the length scale parameter. As shown in "Fig. 11a", with increasing electric field, the tendency to stiffness the system increases, and the natural frequency increases, as the volume power index increases, the mass matrix increases and the natural frequency decreases. But in "Fig. 11b", with the increase of the electric field and the volume power index, the loss factor was first increased and then decreased. As before mentioned, the loss factor is related to material loss factor and strain energy stored, which is first increased and the latter decreases.

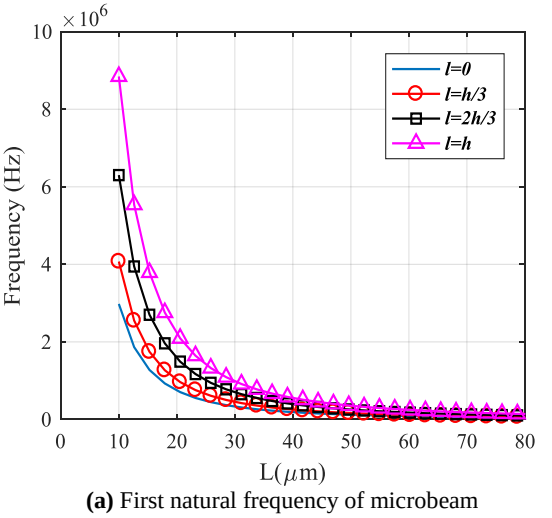

(a) First natural frequency of microbeam

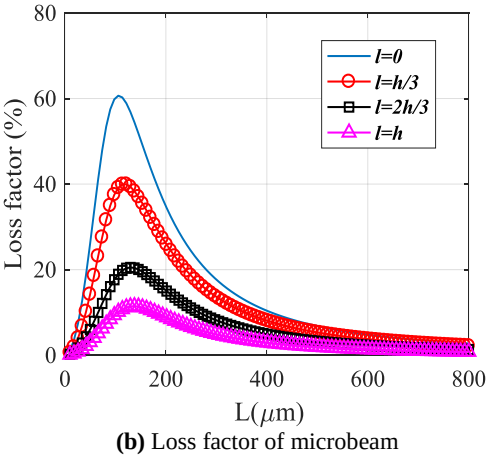

(b) Loss factor of microbeam

Fig. 5 Variation of the natural frequency and loss factor with the length of microbeam for E=1(KV/mm), p=1, q=2 and for various values of the dimensionless length scale parameter.

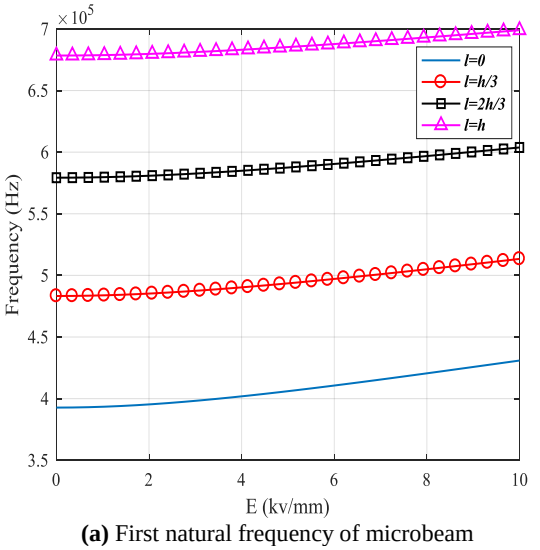

(a) First natural frequency of microbeam

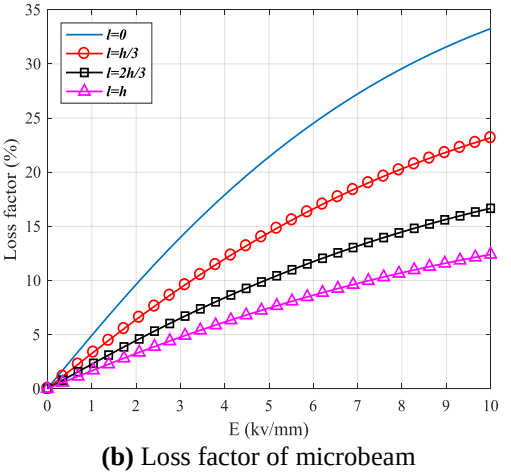

(b) Loss factor of microbeam

Fig. 6 Variation of the natural frequency and loss factor with the electric field for p=1, q=2 and for various values of the length scale parameter.

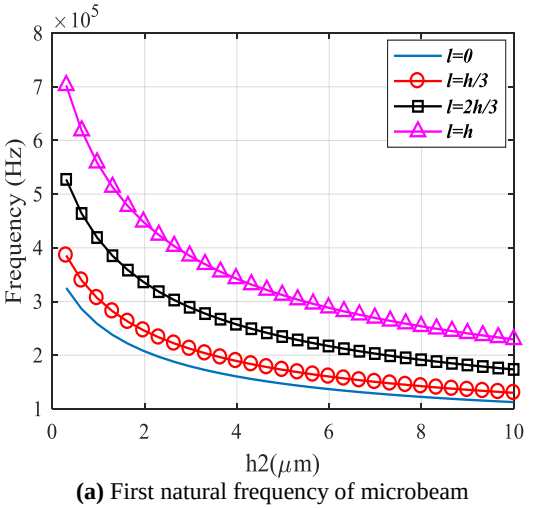

(a) First natural frequency of microbeam

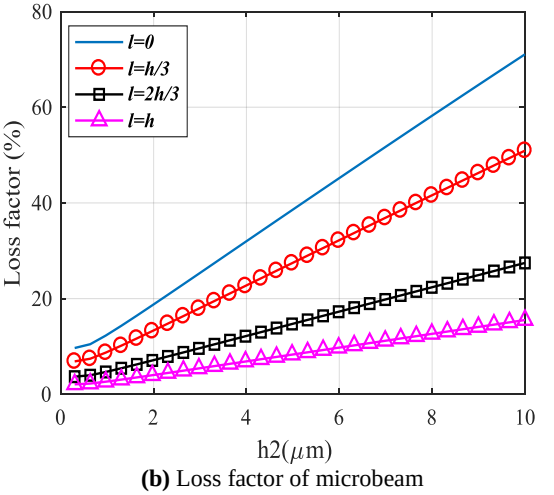

(b) Loss factor of microbeam

Fig. 7 Variation of the natural frequency and loss factor with the thickness of core for E=1(KV/mm), p=1, q=2 and for various values of the dimensionless length scale parameter.

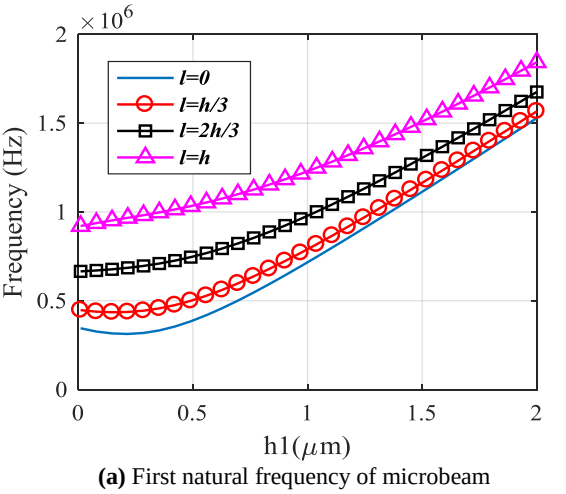

(a) First natural frequency of microbeam

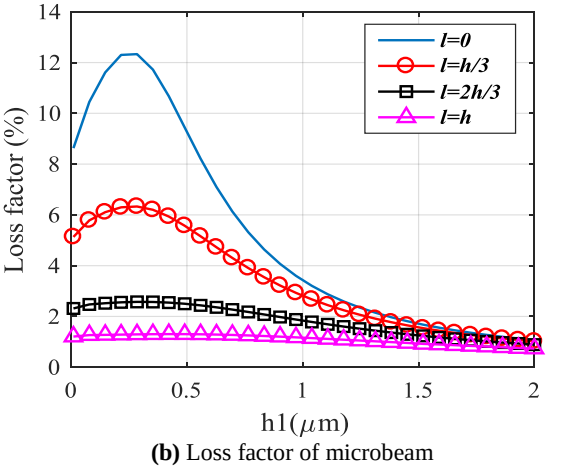

(b) Loss factor of microbeam

Fig. 8 Variation of the natural frequency and loss factor with the thickness of top face for E=1(KV/mm), p=1, q=2, and for various values of the dimensionless length scale parameter.

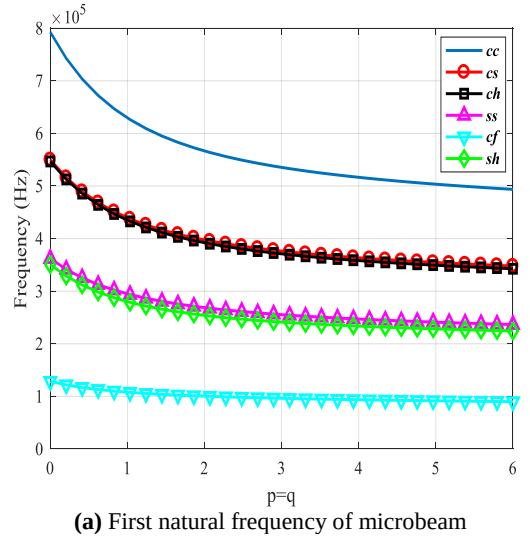

(a) First natural frequency of microbeam

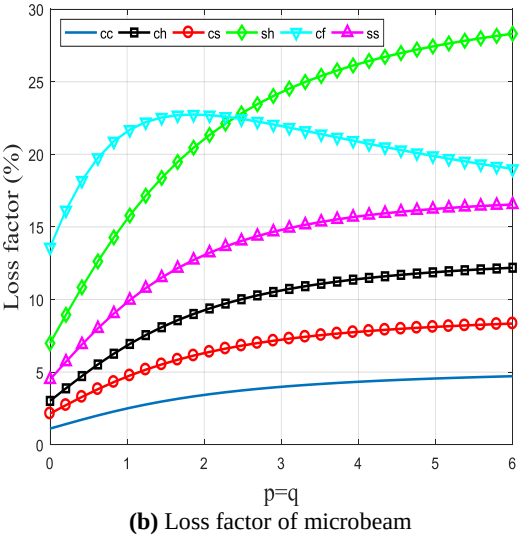

(b) Loss factor of microbeam

Fig. 9 Variation of the natural frequency and loss factor with the volume fractions index for E=1(KV/mm), *l=0.5h* and for various boundary conditions.

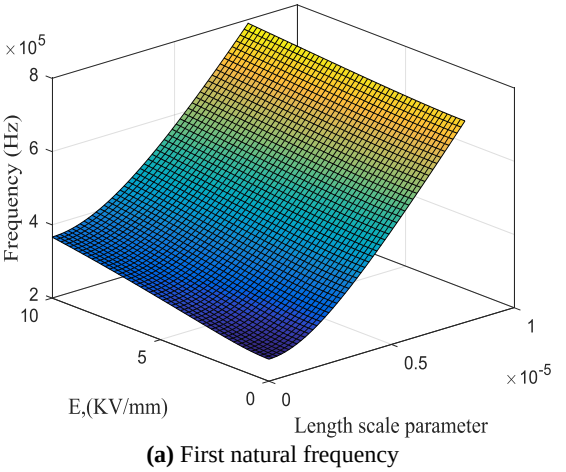

(a) First natural frequency

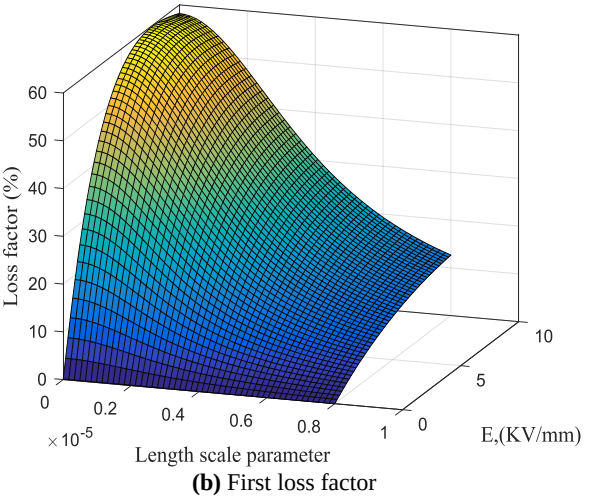

(b) First loss factor

Fig. 10 Variation of the natural frequency and loss factor with the electric field and length scale parameter for, p=1, q=2 and C-S boundary condition.

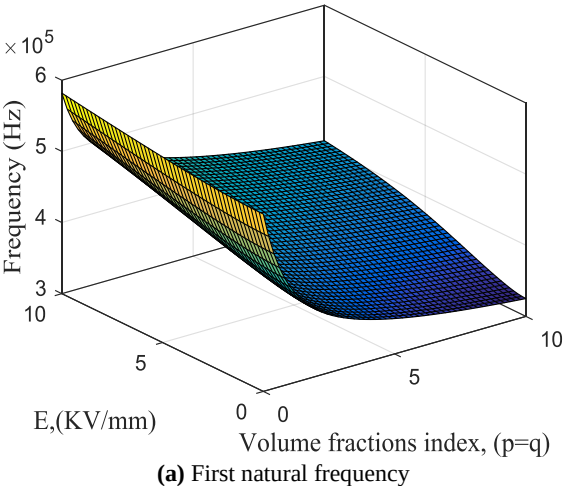

(a) First natural frequency

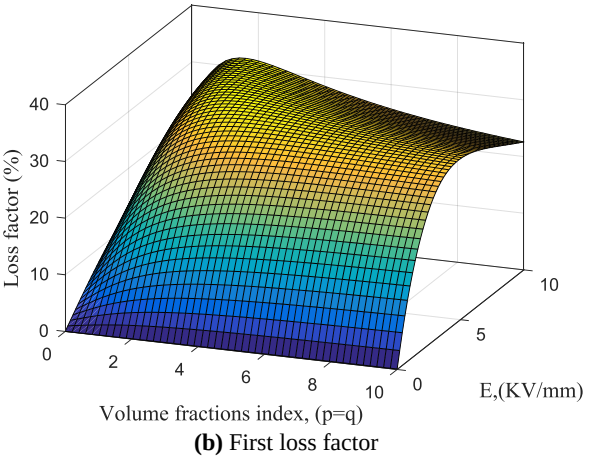

(b) First loss factor

Fig. 11 Variation of the natural frequency and loss factor with the electric field and length scale parameter for p=1, q=2, and C-S boundary condition.

8 FORCED VIBRATIONS

We investigate the microbeam C-F according to "Fig. 1" under dynamic force $F=f_0 sin(\pi x/L)cos(\omega_s t)$. In "Fig 12," we ignore the damping effects in the system and the damping factor in "Eq. (39)" that C=0. By analyzing the response time in "Fig. 12a-b", the noise and disturbance effects on a given system are known, although the range of motion decreases with increasing electric field, it does not have any effect on noise and turbulence. In "Fig. 13", the effects of damping are considered. As seen, there are effects of disturbances until the time t=4s. In "Fig. 14", by inserting the controller on the microbeam and obtaining the optimal gain parameter in feedback, the amplitude, noise and turbulence can be reduced.

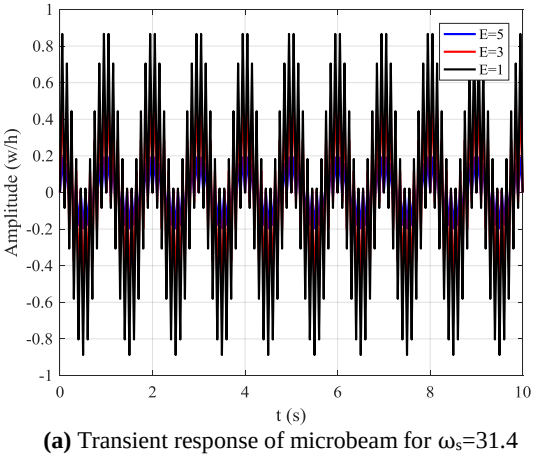

(a) Transient response of microbeam for ω_s=31.4

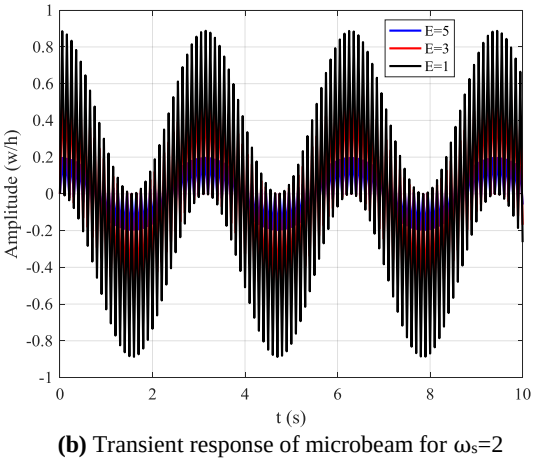

(b) Transient response of microbeam for ω_s=2

Fig. 12 Time history of tip microbeam for, E=1(KV/mm), p=1, q=2, and for various values of the electric field and C-F boundary condition.

In "Fig. 14", the optimum control is placed on the system, using "Eq. (5)" By controlling the electric field, the setting time is equal t=2.2 and t=4.1. The optimal feedback gain values in "Eq. (3)" are k_1=10, k_2=1, k_3=24, k_4=50, k_5=-14.7, k_6=107. In "Fig. 15", the force $F=f_0 sin(\pi x/L)cos(\omega_s t)exp(-2t)$ enters on the microbeam. In "Fig. 15a", damping in the ignition system is considered, but in "Fig. 15b", this damping is considered. In "Fig. 16a", the controller is located on the system and the setting time t=2.6 and maximum oscillation A_0=.18 range are reduced. In "Fig. 16b", the bode diagram was used to indicate the state with controller and no controller.

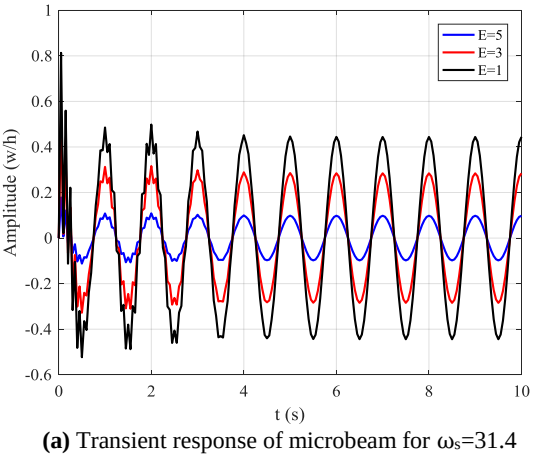

(a) Transient response of microbeam for ω_s=31.4

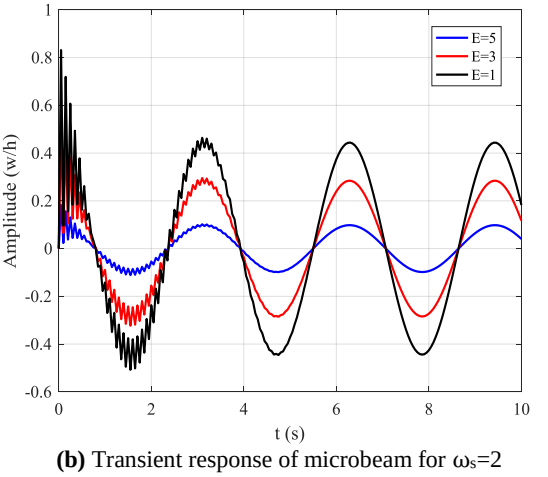

(b) Transient response of microbeam for ω_s=2

Fig. 13 Time history of tip microbeam for, E=1(KV/mm), p=1, q=2, and for various values of the electric field and C-F boundary condition with damping matrix.

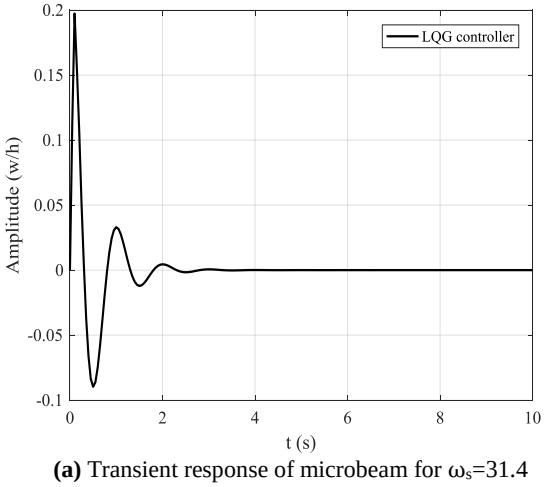

(a) Transient response of microbeam for ω_s=31.4

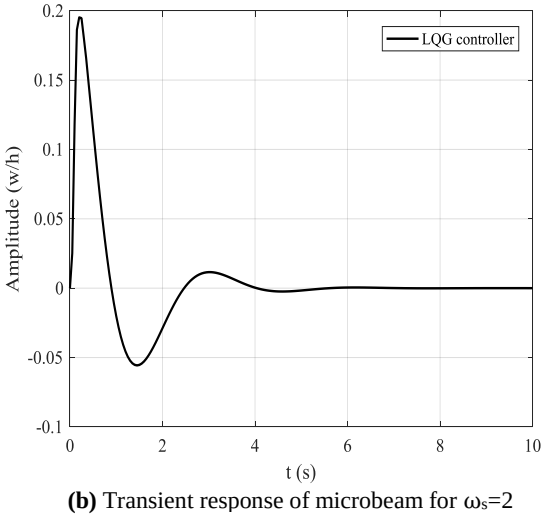

(b) Transient response of microbeam for ω_s=2

Fig. 14 Time history of tip microbeam for, E=1(KV/mm), p=1, q=2, and for various values of the electric field and C-F boundary condition with LQG controller.

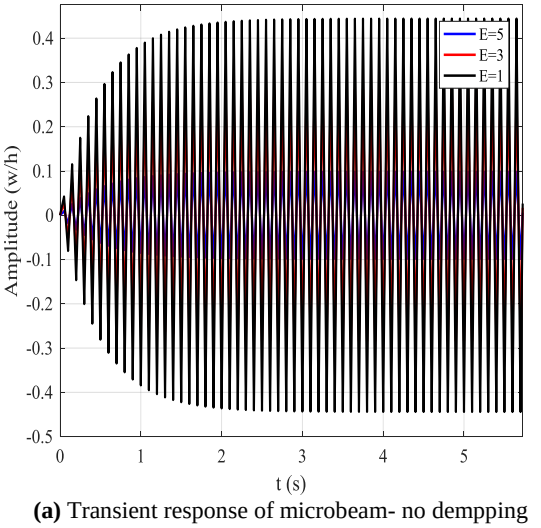

(a) Transient response of microbeam- no dempping

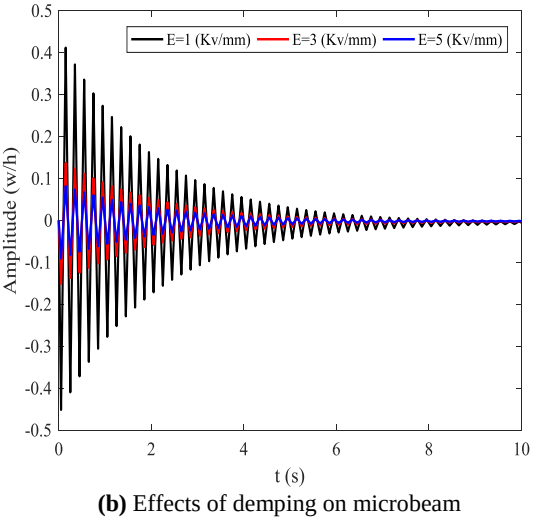

(b) Effects of demping on microbeam

Fig. 15 Comparisons of tip displacement responses of the microbeam with and without damping.

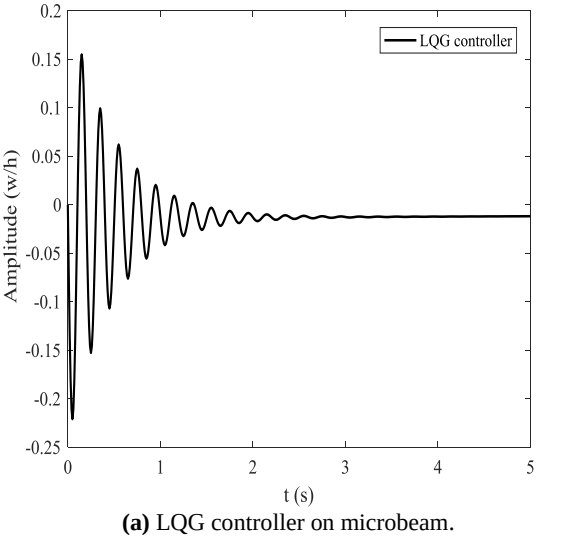

(a) LQG controller on microbeam.

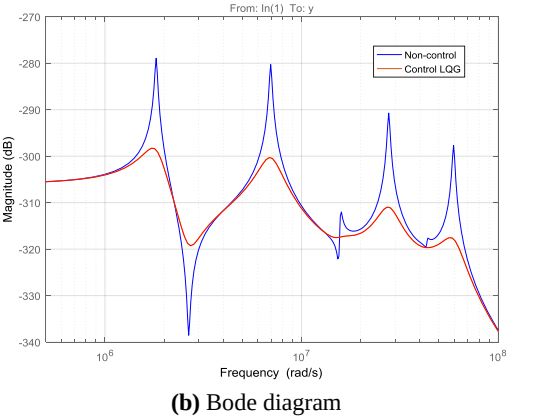

(b) Bode diagram

Fig. 16 The tip deflection responses of the ER sandwich beam with and without the LQG control and subject to a dynamic load

CONCLUSION

In this article, we used the mesh less method of radial basis functions for vibration analysis of sandwich microbeam which showed the effectiveness of this method and the exact answers for free and forced vibrations showed a high convergence rate compared with other numerical methods for various boundary conditions. This method can be combined with other numerical methods such as finite difference. Also, the importance of controller application (LQG) in reduction of transient vibrations was focused on. Combination of RBF method with control methods can be easily done. This method is applicable to all viscoelastic material models. The study shows that with increasing volume fractions index, the natural frequency decreases and the loss factor is increased. As the thickness of the faces, the loss factor is first increased and then reduced. In the case of core, with the increase of the electric field and the core thickness, the natural frequency and loss factor increase simultaneously, due to the increase in system stiffness and the increase of stored strain energy. Also, with the increase in the length scale, parameter of the natural frequency increase and the loss factor decreases. The design of the optimal control feedback on the electric field indicates that there is less setting time and amplitude displacement.

REFERENCES

[1] Ghayesh, M. H., Farokhi, H., and Amabili, M. Nonlinear Dynamics of a Microscale Beam Based on The Modified Couple Stress Theory, Composites Part B: Engineering, Vol. 50, 2013, pp. 318-324.

[2] Gomathi, K., Senthilkumar, A., Shankar, S., Thangavel, S., and Priya, R. M. Hand Arm Vibration Measurement Using Micro-Accelerometer in Different Brick Structures, Smart Structures and Systems., Vol. 13, No. 6, 2014, pp. 959-974.

[3] Mohammadimehr, M., Alimirzaei, S., Buckling and Free Vibration Analysis of Tapered FG-CNTRC Micro-Reddy Beam Under Longitudinal Magnetic Field Using FEM, Smart Structures and Systems., Vol. 19, No. 3, 2017, pp. 309-322.

[4] Asadi, H., Akbarzadeh, A. H., and Wang, Q., Nonlinear Thermo-Inertial Instability of Functionally Graded Shape Memory Alloy Sandwich Plates, Composite Structures, Vol. 120, 2015, pp. 496-508.

[5] Yeh, J. Y., Parametric Resonance of Axisymmetric Sandwich Annular Plate with Er Core Layer and Constraining Layer, Smart Structures and Systems, Vol. 8, No. 5, 2011, pp. 487-499.

[6] El Wahed, A. K., Balkhoyor, L. B., Magnetorheological Fluids Subjected to Tension, Compression, and Oscillatory Squeeze Input, Smart Structures and Systems., Vol. 16, No. 5, 2015, pp. 961-980.

[7] Yalcintas, M., Coulter, J. P., Electrorheological Material Based Adaptive Beams Subjected to Various Boundary Conditions, Journal of Intelligent Material Systems and Structures, Vol. 6, No. 5, 1995, pp. 700-717.

[8] Arikoglu, A., Ozkol, I., Vibration Analysis of Composite Sandwich Beams with Viscoelastic Core by Using Differential Transform Method, Composite Structures, Vol. 92, No. 12, 2010, pp. 3031-3039.

[9] Rahn, C. D., Joshi, S., Modeling and Control of An Electrorheological Sandwich Beam, Journal of vibration and acoustics, Vol. 120, No. 1, 1998, pp. 221-227.

[10] Rezaeepazhand, J., Pahlavan, L., Transient Response of a Three-Layer Sandwich Plate with Electrorheological Core and Orthotropic Faces, In 13th European Conference on Composite Materials-ECCM, Vol. 13, 2008.

[11] Adessina, A., Hamdaoui, M., and Xu, C., Damping Properties of Bi-Dimensional Sandwich Structures with Multi-Layered Frequency-Dependent Visco-Elastic Cores, Composite Structures, Vol. 154, 2016, pp. 334-343.

[12] Bhangale, R. K., Ganesan, N., Thermoelastic Buckling and Vibration Behavior of a Functionally Graded Sandwich Beam with Constrained Viscoelastic Core, Journal of Sound and Vibration, Vol. 295, No. 1, 2006, pp. 294-316.

[13] Allahverdizadeh, A., Mahjoob, M. J., Eshraghi, I., and Nasrollahzadeh, N., On the Vibration Behavior of Functionally Graded Electrorheological Sandwich Beams, International Journal of Mechanical Sciences, Vol. 70, 2013, pp. 130-139.

[14] Allahverdizadeh, A., Eshraghi, I., Mahjoob, M. J., and Nasrollahzadeh, N., Nonlinear Vibration Analysis of FGER Sandwich Beams, International Journal of Mechanical Sciences, Vol. 78, 2014, pp. 167-176.

[15] Vasques, C. M. A., Rodrigues, J. D., Combined Feedback/Feedforward Active Control of Vibration of Beams with ACLD Treatments: Numerical Simulation, Computers & Structures., Vol. 86, No. 3, 2008, pp. 292-306.

[16] Hansen, C. H., Snyder, S. D., Active Control of Sound and Vibration, E&FN Spon, London, 1997.

[17] Benjeddou, A., Advances in Hybrid Active-Passive Vibration and Noise Control Via Piezoelectric and Viscoelastic Constrained Layer Treatments, Journal of Vibration and Control., Vol. 7, No. 4, 2001, pp. 565-602.

[18] Friswell, M. I., Inman, D. J., The Relationship Between Positive Position Feedback and Output Feedback Controllers, Smart Materials and Structures., Vol. 8, No. 3, 1999, pp. 285.

[19] Meirovitch, L., Baruh, H., Control of Self-Adjoint Distributed-Parameter Systems, Journal of Guidance, Vol. 5, No. 1, 1982, 60-66.

[20] Hanagud, S., Obal, M. W., and Calise, A. J., Optimal Vibration Control by The Use of Piezoceramic Sensors and Actuators, Journal of Guidance, Control, and Dynamics, Vol. 15, No. 5, 1992, pp. 1199-1206.

[21] Kwakernaak, H., Sivan, R., Linear Optimal Control Systems, New York: Wiley-Interscience, 1972.

[22] Eringen, A. C., Nonlocal Continuum Field Theories, Springer Science & Business Media, 2002.

[23] Ebrahimi, F., Shafiei, N., Application of Eringens Nonlocal Elasticity Theory for Vibration Analysis of Rotating Functionally Graded Nanobeams", Smart Structures and Systems, Vol. 17, No. 5, 2016, pp. 837-857.

[24] Shen, J. P., Li, C., Fan, X. L., and Jung, C. M., Dynamics of Silicon Nanobeams with Axial Motion Subjected to Transverse and Longitudinal Loads Considering Nonlocal and Surface Effects, Smart Structures and Systems, Vol. 19, No. 1, 2017.

[25] Ebrahimi, F., Salari, E., Semi-Analytical Vibration Analysis of Functionally Graded Size-Dependent Nanobeams with Various Boundary Conditions, Smart Structures and Systems, Vol. 19, No. 3, 2017, pp. 243-257.

[26] Gurtin, M. E., Weissmüller, J., and Larche, F., A General Theory of Curved Deformable Interfaces in Solids at Equilibrium, Philosophical Magazine A., Vol 78, No. 5, 1998, pp. 1093-1109.

[27] Eringen, A. C., Theory of Micropolar Plates, Zeitschrift für Angewandte Mathematik und Physik (ZAMP), Vol. 18, No. 1, 1967, pp. 12-30.

[28] Mindlin, R. D., Influence of Couple-Stresses on Stress Concentrations, Experimental Mechanics, Vol. 3, No. 1, 1963, pp. 1-7.

[29] Aifantis, E. C., Strain Gradient Interpretation of Size Effects, International Journal of Fracture., Vol. 95, No. 1, 1999, pp. 299-314.

[30] Ghorbanpour Arani, A., Kolahchi, R., and Esmailpour, M., Nonlinear Vibration Analysis of Piezoelectric Plates Reinforced with Carbon Nanotubes Using DQM, Smart Structures and Systems, Vol. 18, No. 4, 2016, pp. 787-800.

[31] Mohammadimehr, M., Monajemi, A. A., Nonlinear Vibration Analysis of MSGT Boron-Nitride Micro Ribbon Based Mass Sensor Using DQEM, Smart Structures and Systems, Vol. 18, No. 5, 2016, pp. 1029-1062.

[32] Yang, F. A. C. M., Chong, A. C. M., Lam, D. C. C., and Tong, P., Couple Stress Based Strain Gradient Theory for Elasticity, International Journal of Solids and Structures., Vol. 39, No, 10, 2002, pp. 2731-2743.

[33] Şimşek, M., Reddy, J. N., Bending and Vibration of Functionally Graded Microbeams Using a New Higher Order Beam Theory and The Modified Couple Stress Theory, International Journal of Engineering Science, Vol. 64, 2013, pp. 37-53.

[34] Akbas, S. D., Forced Vibration Analysis of Viscoelastic Nanobeams Embedded in An Elastic Medium, Smart Structures and Systems, Vol. 18, No. 6, 2016, pp. 1125-1143.

[35] Roque, C. M. C., Martins, P. A. L. S., Ferreira, A. J. M., and Jorge, R. M. N., Differential Evolution for Free Vibration Optimization of Functionally Graded Nano Beams, Composite Structures, Vol. 156, 2016, pp. 29-34.

[36] Şimşek, M., Size Dependent Nonlinear Free Vibration of An Axially Functionally Graded (AFG) Microbeam Using He's Variational Method, Composite Structures., Vol. 131, 2015, pp. 207-214.

[37] Akgöz, B., Civalek, Ö., Free Vibration Analysis of Axially Functionally Graded Tapered Bernoulli–Euler Microbeams Based on The Modified Couple Stress Theory, Composite Structures, Vol. 98, 2013, pp. 314-322.

[38] Arefi, M., Pourjamshidian, M., and Ghorbanpor Arani, A., Nonlinear free and forced vibration analysis of embedded Functionally Graded Sandwich Micro Beam with Moving Mass, Journal of Sandwich Structures & Materials., 2016, 1099636216658895.

[39] Asemi, K., Salami, S. J., Salehi, M., and Sadighi, M., Dynamic and Static Analysis of FGM Skew Plates with 3D Elasticity Based Graded Finite Element Modeling, Latin American Journal of Solids and Structures, Vol. 11, No. 3, 2014, pp. 504-533.

[40] Ghorbanpour Arani, A., Kolahchi, R., Mosayyebi, M., and Jamali, M., Pulsating Fluid Induced Dynamic Instability of Visco-Double-Walled Carbon Nano-Tubes Based on Sinusoidal Strain Gradient Theory Using DQM and Bolotin Method, International Journal of Mechanics and Materials in Design, Vol. 12, No. 1, 2016, pp. 17-38.

[41] Garshasbi, M., Khakzad, M., The RBF Collocation Method of Lines for The Numerical Solution of the CH−γ Equation, Journal of Advanced Research in Dynamical and Control Systems, Vol. 7, No. 4, 2015, pp. 65-83.

[42] Shu, C., Ding, H., and Yeo, K. S. Solution of Partial Differential Equations by A Global Radial Basis Function-Based Differential Quadrature Method, Engineering Analysis with Boundary Elements, Vol. 28, No. 10, 2004, pp. 1217-1226.

[43] Dehrouyeh-Semnani, A. M., Dehrouyeh, M., Torabi-Kafshgari, M., and Nikkhah-Bahrami, M., An Investigation into Size-Dependent Vibration Damping Characteristics of Functionally Graded Viscoelastically Damped Sandwich Microbeams, International Journal of Engineering Science, Vol. 96, 2015, pp. 68-85.